Electronic Supplementary Material (ESI) for Energy Advances.

Supplementary Information – Rapid sintering of $Li_{6.5}La_3Zr_1Nb_{0.5}Ce_{0.25}Ti_{0.25}O_{12}$ for high density lithium garnet electrolytes with current induced *in-situ* interfacial resistance reduction.

M. P. Stockham[1*], B. Dong[1,3], M.S. James[1], P. Zhu[2,3], E. Kendrick[2,3], P.R. Slater[1,3]*

[1]School of Chemistry, University of Birmingham, Birmingham B15 2TT. UK

[2]School of Metallurgy and Materials, University of Birmingham, Birmingham B15 2TT. UK

[3]The Faraday Institution, Quad One, Harwell Campus, Didcot OX11 0RA, UK

Correspondence to

M. P. Stockham/P. R. Slater

School of Chemistry, University of Birmingham, Birmingham B15 2TT. UK

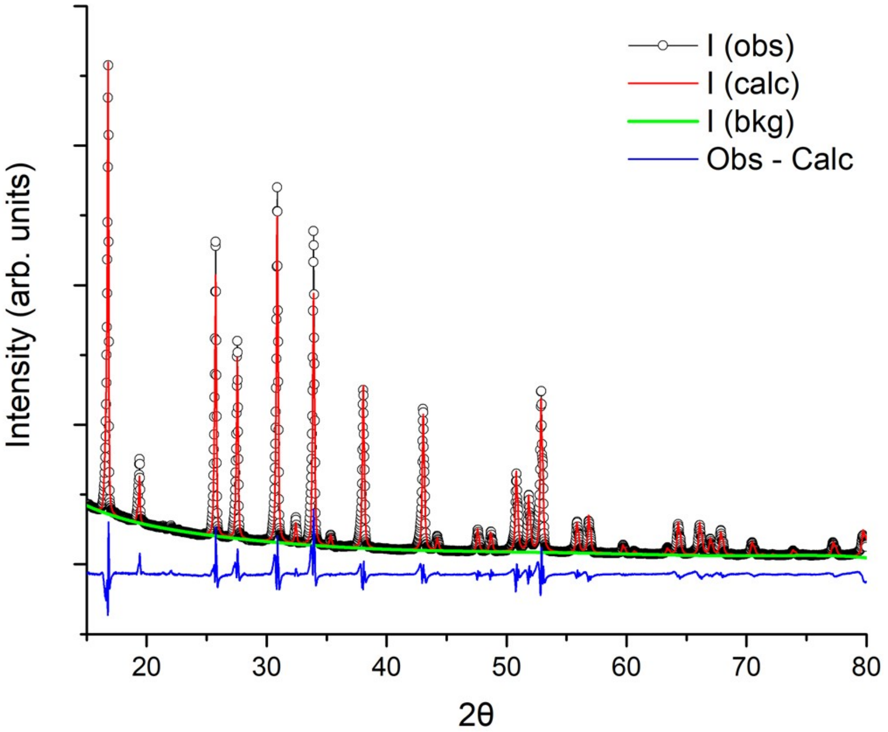

Figure S1. Example Rietveld refinement showing the Observed, calculated and difference profiles. R_{wp} = 9.79 %.

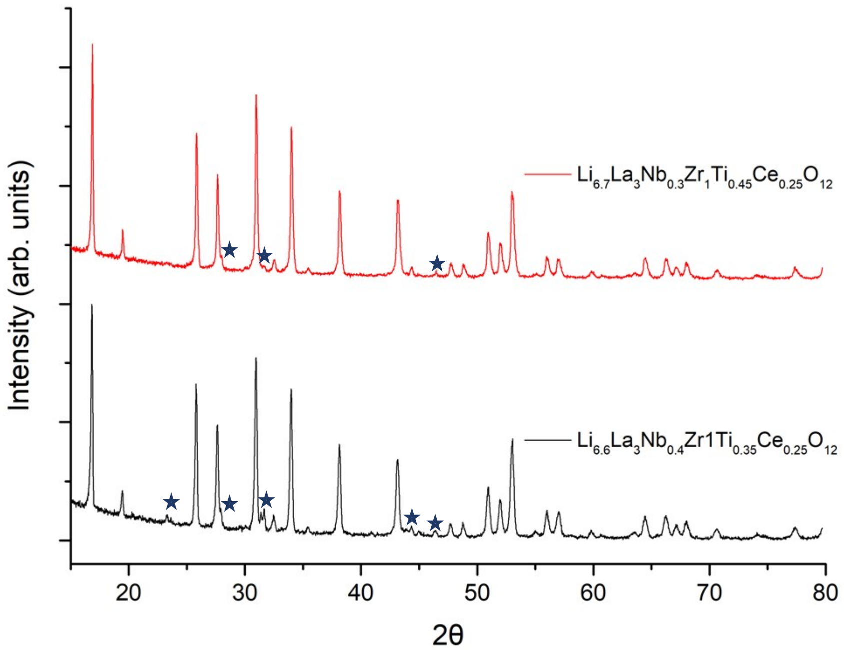

Figure S2 XRD patterns of $Li_{6.6}La_3Nb_{0.4}Zr_1Ti_{0.35}Ce_{0.25}O_{12}$ and $Li_{6.7}La_3Nb_{0.3}Zr_1Ti_{0.45}Ce_{0.25}O_{12}$ showing CeO_2 and Ce_4O_7 impurities marked with blue stars.

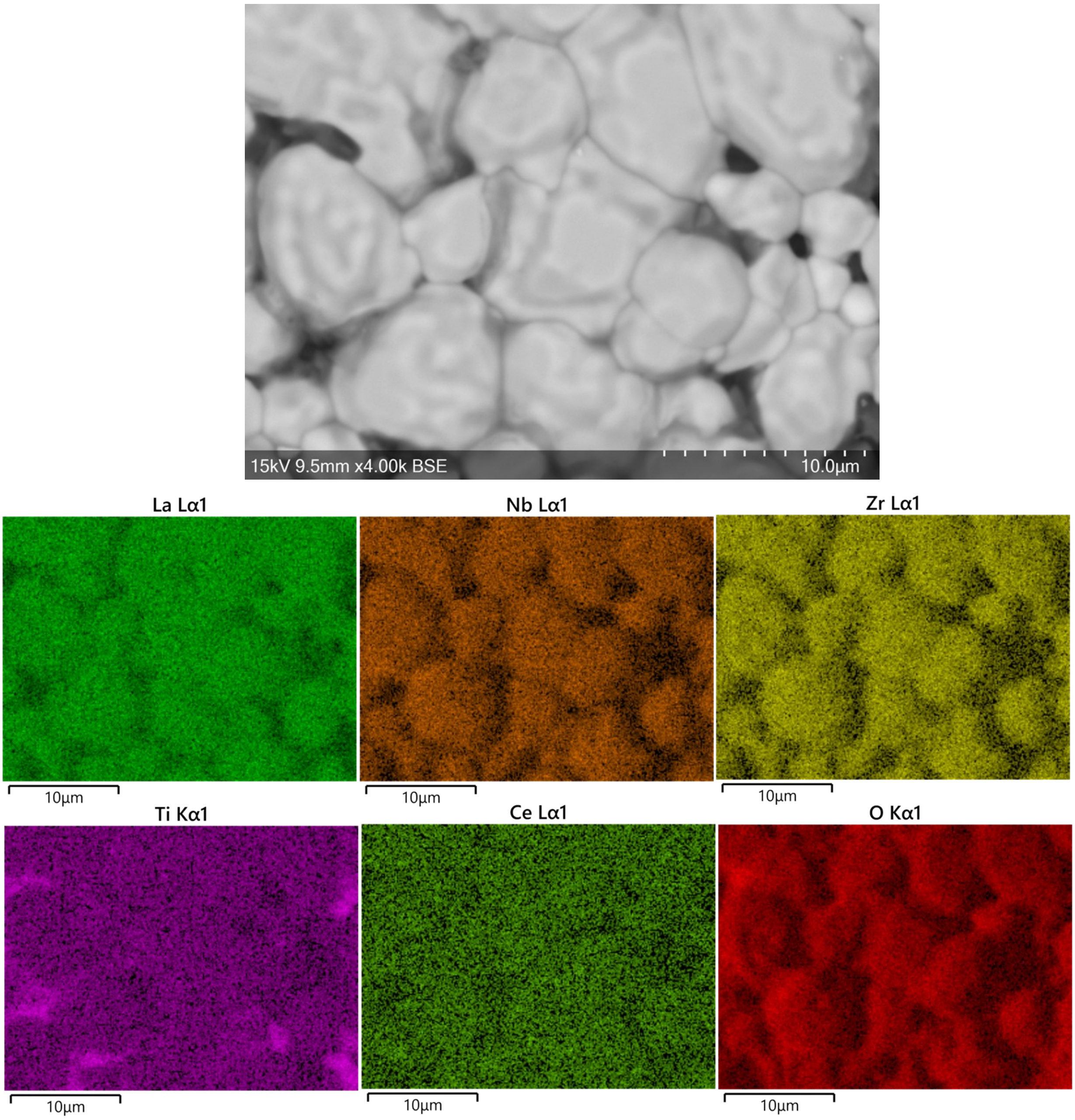

Figure S3. SEM of unpolished pellet surface sintered at 1100°C with corresponding EDX of pellet surface. The pellet was unpolished to allow for clearer imaging of individual grains, therefore enabling clearer composition analysis per grain. EDX images shown relatively homogenous elemental distribution but with additional Ti contributions in the more porous areas of the surface, as discussed in the main article.

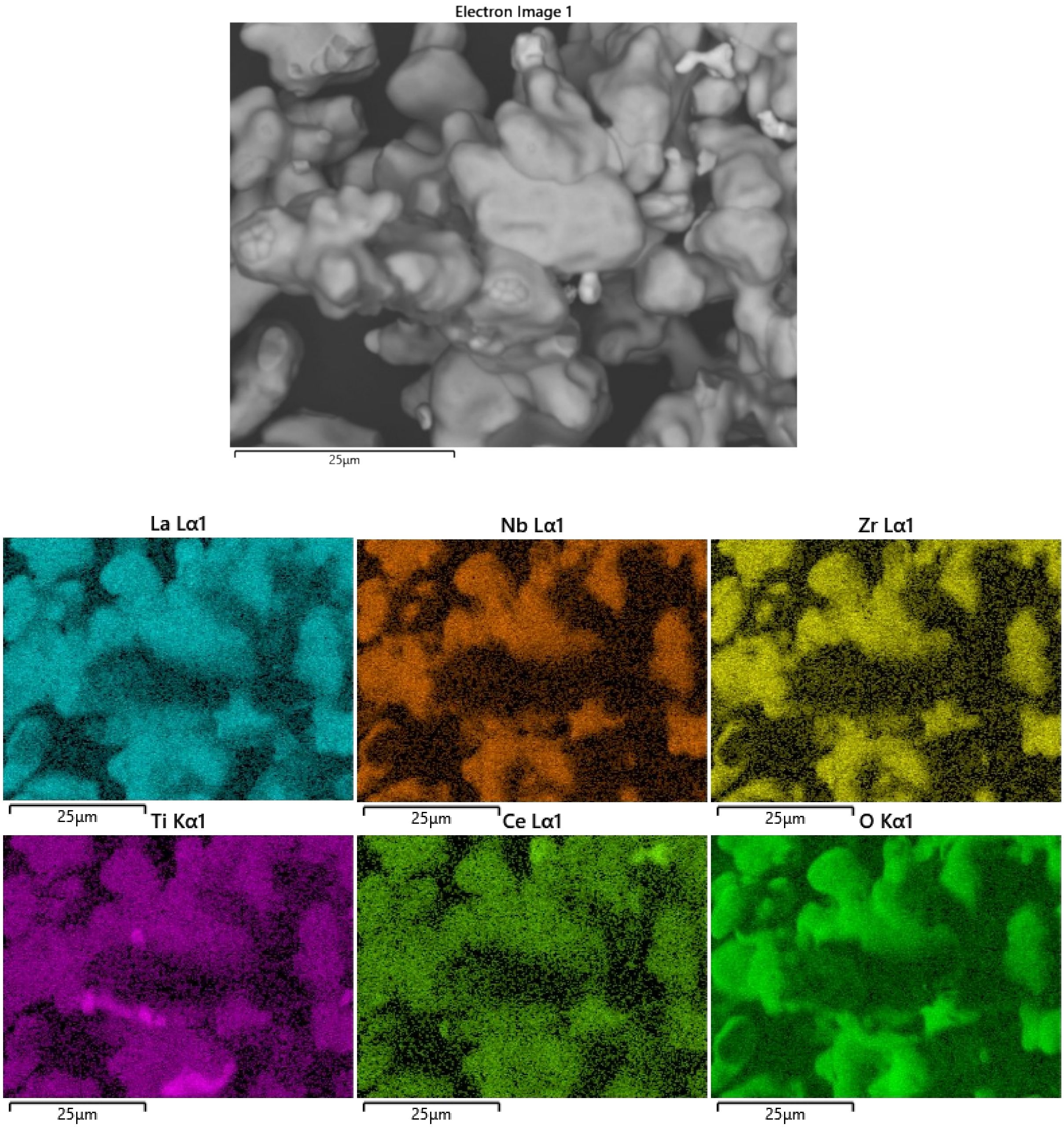

Figure S4. SEM and EDX of LTC powder synthesised at 950°C with corresponding EDX of pellet surface. EDX images shown relatively homogenous elemental distribution but with additional Ti contributions near the edges of some grains, as discussed in the main article. Darkened areas relate to sample orientation.

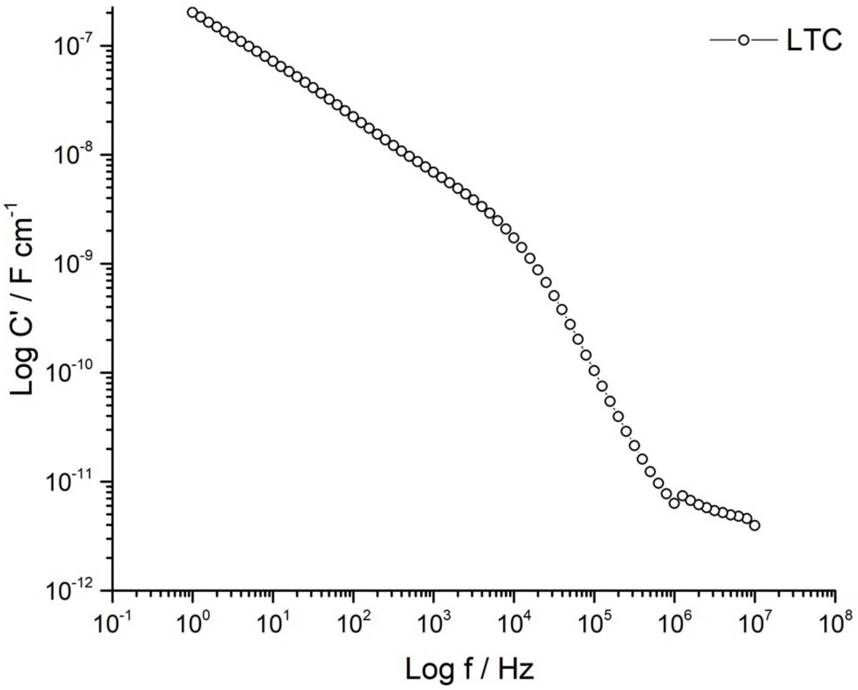

Figure S5. Spectroscopic C plot of LTC with Au blocking electrodes at 22°C, showing a high frequency plateau at 4.79 x10^{-12} F cm^{-1}. This corresponds to the expected values for a bulk contribution, as seen in table 1 in the main article.

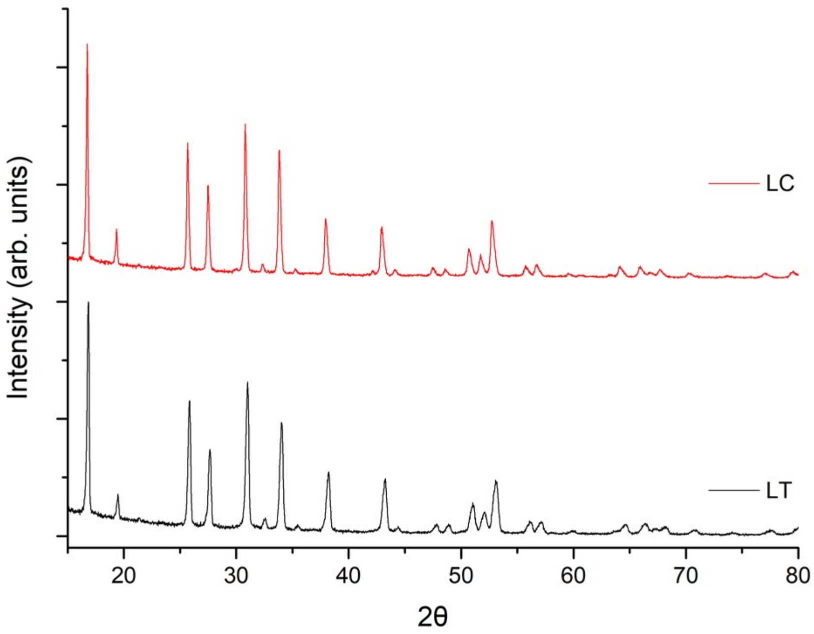

Figure S6. XRD patterns of LT and LC, both showing pure phases indexed on *Ia*$\bar{3}$*d* type symmetry

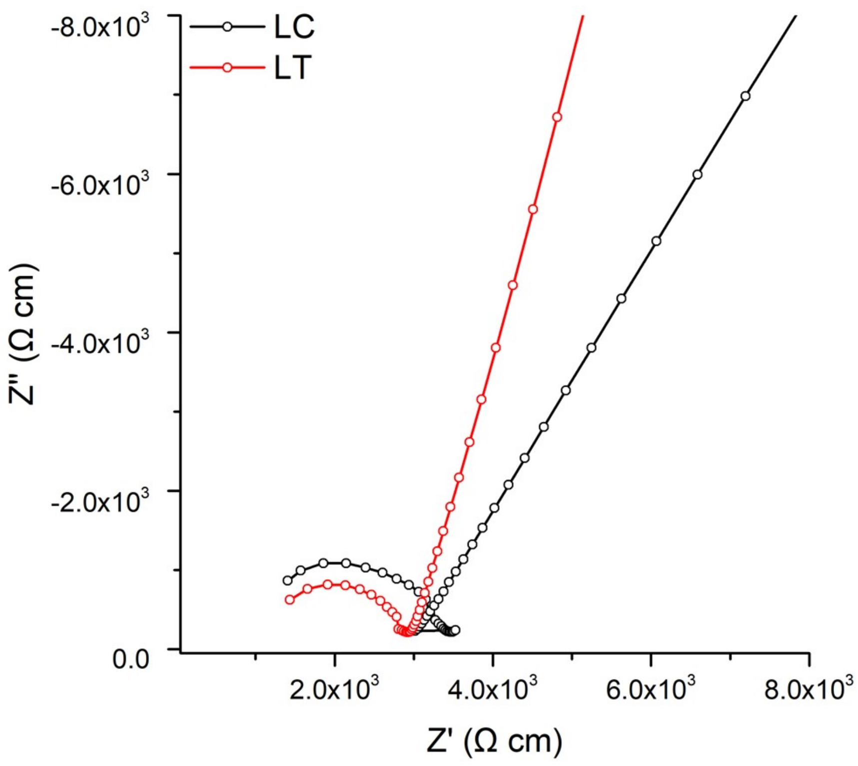

Figure S7. Impedance spectra of LT and LC showing high conductivity at room temperature. The change in spectrum for LC, in the mid frequency, range is associated to experimental equipment error.

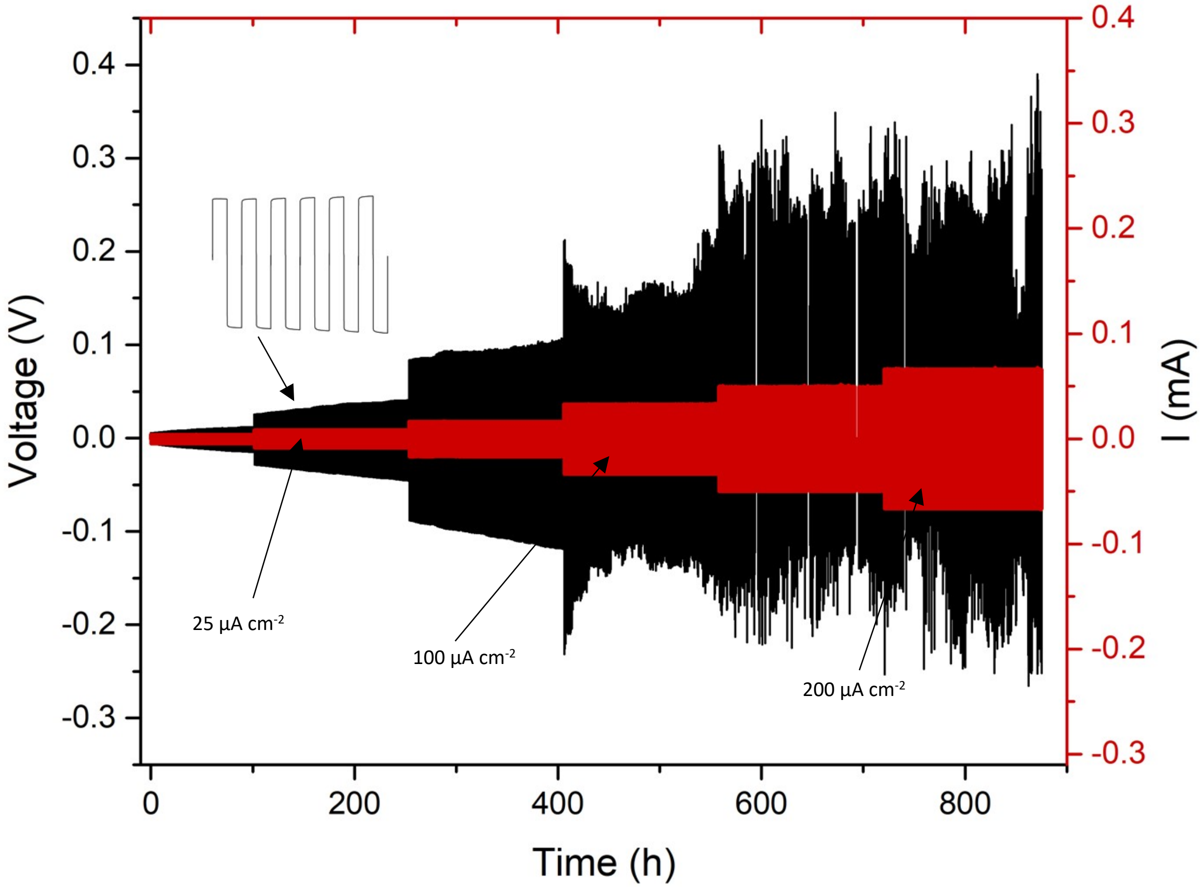

Figure S8. Long term cycling of an Li/LTC/Li symmetrical cell at 49°C. Lower current densities have mostly flat voltage profiles and show stable cycling behaviour. Higher current densities still do not show a large reduction in voltage, indicative of a short circuit, however, show the erratic voltage profiles described in the main article. Gaps in voltage profile indicate where cell was stopped for impedance analysis, which showed no clear short circuit. The cell had an ASR of 576 Ω cm^2. This enabled the unusual Li dendrite phenomena to be observed more rapidly, thus starting at 100 µA cm^{-2} rather than ~140 µA cm^{-2} , as seen in the main article.

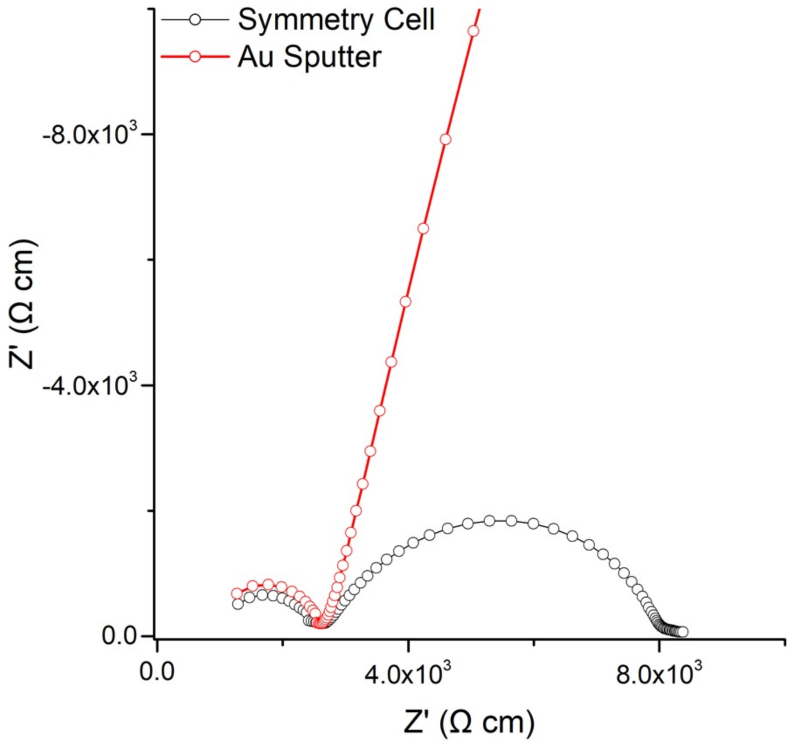

Figure S9. An overlaid impedance spectrum of the pristine LTC symmetrical cell and Au sputtered pellet, to confirm the correct assignment of the low frequency semi-circle to the Li/LTC metal interface.

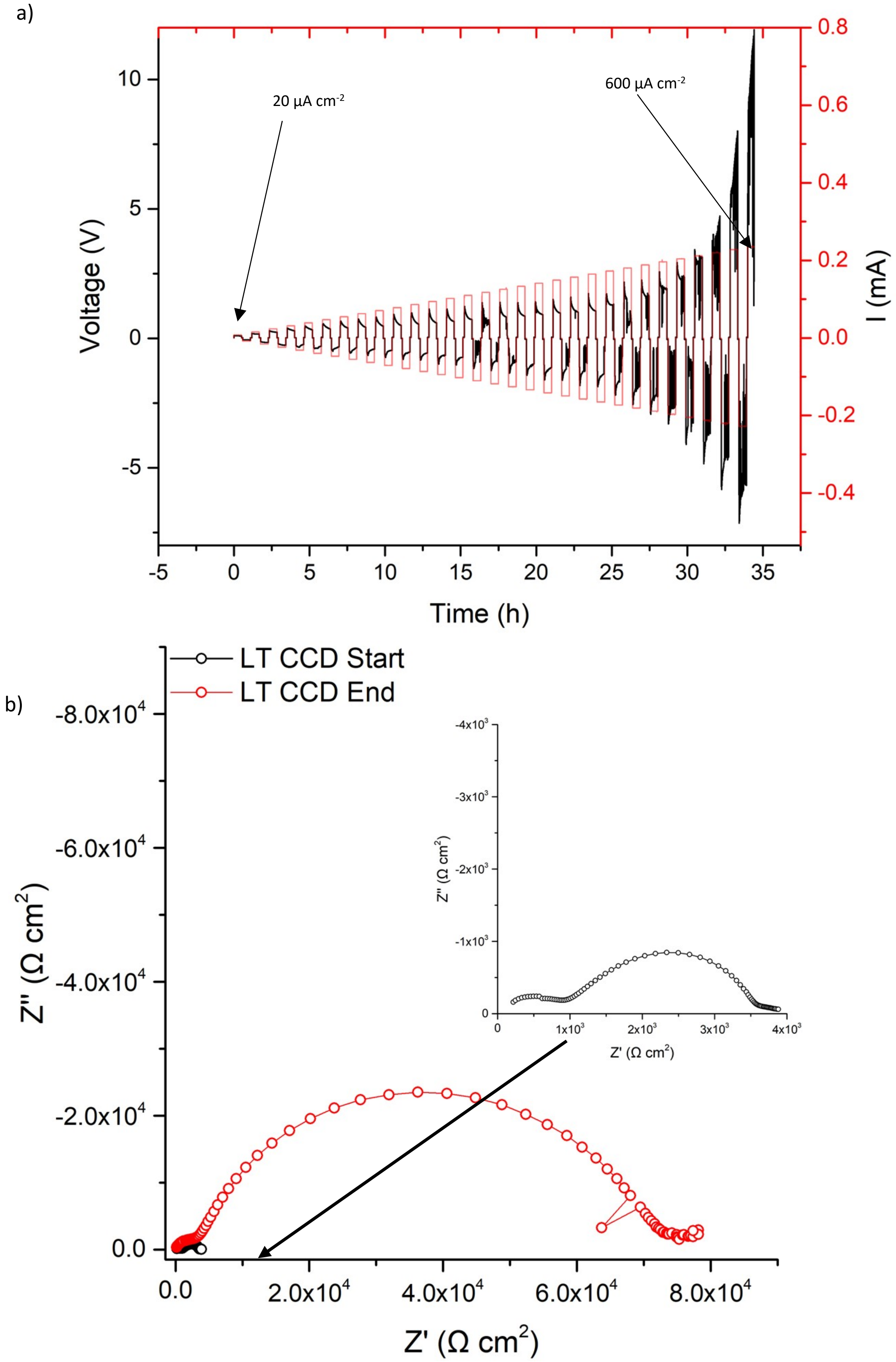

Figure S10. a) CCD analysis of LT garnets in increments of 20 μA cm^{-2} (starting at 20 μA cm^{-2}). b) Impedance spectra of LTC at the start and upon the voltage spike to 10 V, which automatically stopped the tester. Inlay is the original LT spectrum prior to interfacial breakdown.

a)

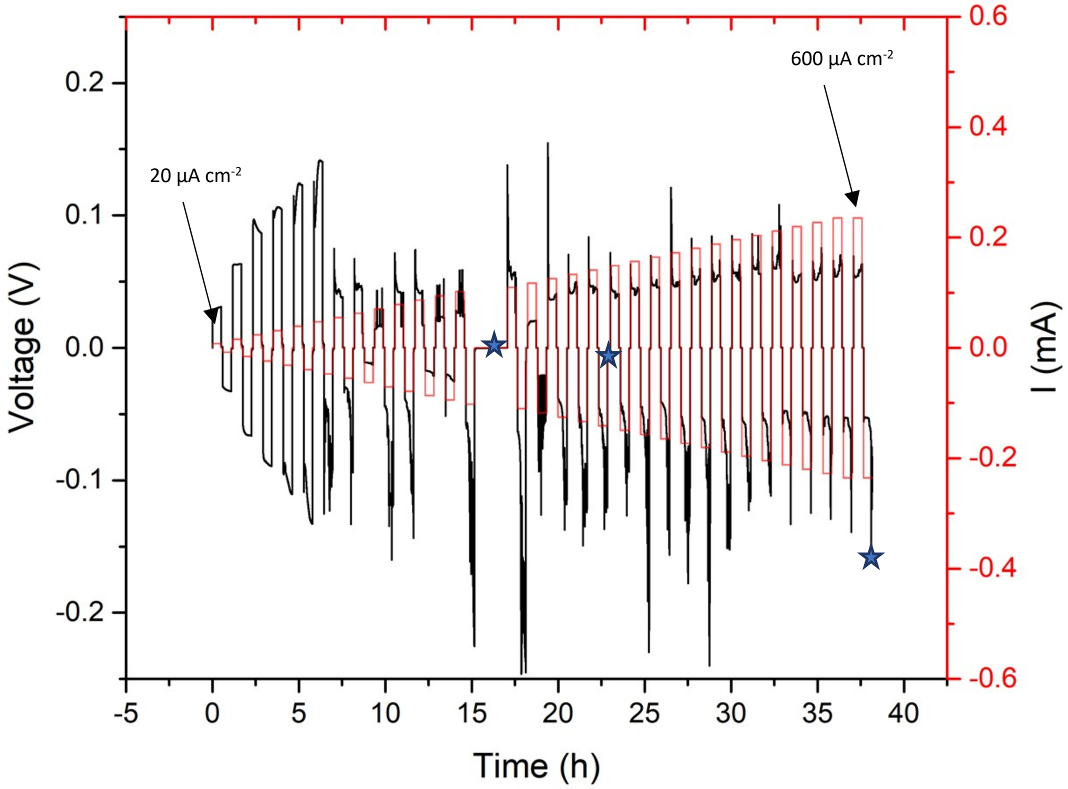

b)

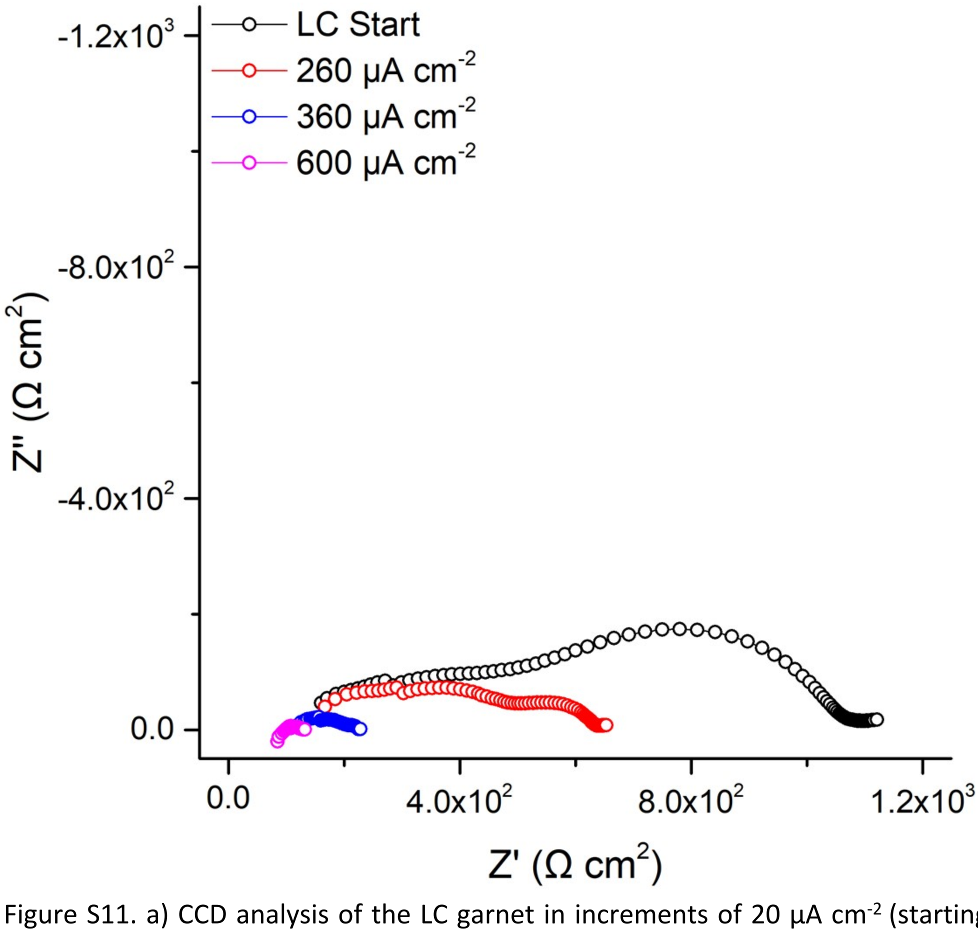

Figure S11. a) CCD analysis of the LC garnet in increments of 20 µA cm^{-2} (starting at 20 µA cm^{-2}). Stars indicate where the cell was stopped for corresponding impedance measurements seen in b).